Two-photon absorption in direct bandgap semiconductors quantum dots

Lazaro A. Padilha*[a,b], Jie Fu[a], G. Nootz[a], David J. Hagan[a,c], Eric W. Van Stryland[a,c], D. Buso[d], A. Martucci[d], Carlos L. Cesar[b], Luiz C. Barbosa[b], and Carlos H. B. Cruz[b]
[a] College of Optics and Photonics: CREOL & FPCE, University of Central Florida, 4000 Central Florida Blvd, Orlando, FL 32816
[b] Instituto de Física "Gleb Wataghin", Universidade Estadual de Campinas, Campinas-SP, Brazil 13083-970
[c] Department of Physics, University of Central Florida, 4000 Central Florida Blvd, Orlando, FL 32816
[d]Dipartimento de Ingegneria Meccanica – Settore Materiali, Universitá di Padova, via Marzolo, 9, I-35131 Padova, Italy

ABSTRACT

We present degenerate and nondegenerate two-photon absorption spectra in a series of CdSe and CdTe quantum dots. The measurements show that the two-photon absorption (2PA) spectrum is strongly dependent on the quantum dot size and that the 2PA coefficient decreases as the quantum dot size decreases, and it is larger for the frequency nondegenerate process. Previously we had shown a theoretical analysis of these results based on a simple model using the effective mass approximation. Although this model works well for larger quantum dots, it fails for the smaller ones. Here we use the more realistic $\vec{k} \bullet \vec{p}$ model for the band structure and consider the hole band mixing in quantum dots to describe our data. This theory better describes the spectral structures for smaller quantum dots and also predicts the decrease of the 2PA coefficient with the decrease of quantum dot size. This is due to the reduction of the number of possible transitions and the blue shift of the optical bandgap from quantum confinement. This theory predicts the reduction of the 2PA coefficient with size, although our experimental results show an even stronger reduction.

Keywords: Semiconductor quantum dots, nonlinear optics, two-photon absorption, nonlinear spectroscopy.

1. INTRODUCTION

Quantum-confined semiconductors have attracted increasing attention owing to reports that they are good candidates for applications in different areas such as biological markers[1,2], all-optical switching[3,4], and quantum computing[5]. Among the quantum-confined semiconductors, special interest has been directed to the ones with 3-dimensional confinement, the quantum dots (QDs). The possibility of changing the quantum dot properties by controlling their size and size distribution allows for tunable optical proprieties so that they can be applied in devices from the ultraviolet to the infrared.

The influence of quantum confinement and the quantum dot size on the linear optical properties is well understood: the linear absorption edge is blue-shifted and the blue shift depends on the QD size; its spectrum exhibits peaks in the resonance energies with peak positions also determined by the QD size. Sercel and Vahala have proposed the widely used theory for describing the electronic structure in these nanocrystals by considering the mixing between the valence bands[6]. On the other hand, many aspects of the nonlinear optical properties are not fully understood, such as the influence of the quantum dot size on the spectral behavior of the real and imaginary parts of the third-order

Nanoengineering: Fabrication, Properties, Optics, and Devices III
edited by Elizabeth A. Dobisz, Louay A. Eldada, Proc. of SPIE Vol. 6327
63270M, (2006) · 0277-786X/06/$15 · doi: 10.1117/12.681160

susceptibility, $\chi^{(3)}$. Until now, many authors have reported different results for these properties in QDs, and when compared to bulk semiconductors, in QDs some authors have reported higher values for the nonlinear refractive index, n_2, which corresponds to the real part of $\chi^{(3)}$, and lower values for the t2PA coefficient, β, which corresponds to the imaginary part of $\chi^{(3)}$ [7,8]. Nevertheless, other authors have reported both n_2 and β as being nearly the same as for bulk semiconductors.[9]

Recently we have reported the frequency degenerate and nondegenerate 2PA spectra in different sizes of CdTe quantum dots in borosilicate glass matrices[10]. In that paper it was shown that the spectra, both the degenerate and nondegenerate, strongly depend on the QD size. We also showed that the maximum value of the 2PA cross-section decreases for smaller nanocrystals[11]. For the previous data, a simple theory, based on the parabolic band model[12] was proposed for fitting the 2PA spectra[10]. That theory fit the data well for larger QDs, however it was important to consider a more realistic theory for describing the 2PA in smaller QDs[10,11]. In the present paper, we discuss the degenerate and nondegenerate 2PA for different sizes of CdSe and CdTe QDs measured by single wavelength Z-scan[13], pump-probe with white-light continua[14] (WLC), and two photon fluorescence[15](2PF) methods. A more complete theory considering the mixing of the light and heavy holes bands (from $\vec{k} \bullet \vec{p}$ theory) is used to explain the 2PA spectra.

2. EXPERIMENT

2.1 Samples

The CdTe QDs samples are dispersed in borosilicate glass. They are fabricated by the melting technique,[16] where the host glass components are melted together (CdO and metallic Te), and then, after the casting process, the glass is heat treated. The time and temperature of the heat treatment determine the QD size and size distribution. Here we present data on two different samples, CdTe-750, which contains QDs with radii of 6.6 ± 0.9 nm, and the first peak in the linear absorption spectra at 750 nm (E_g = 1.67 eV) with a fill fraction of 0.85%, and CdTe-600, with QDs of radii 3.2 ± 0.2 nm, and a first linear absorption peak at 600nm (E_g = 2.07 eV), with a fill fraction of 2.0%. Figure 1 shows the linear absorption spectrum for the two samples.

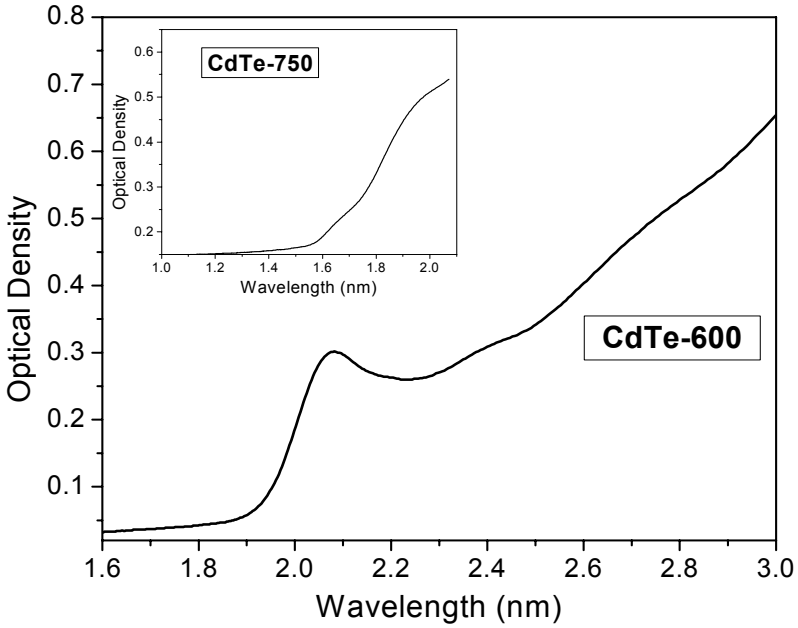

Fig. 1 Linear absorption spectra for CdTe-750 and CdTe-600. Due to the broad distribution size in CdTe-750 the first exciton peak is not clear

The CdSe samples are colloidal quantum dots dispersed in Methanol and Octadecene. The synthesis of CdSe quantum dots was realized according to a slightly modified procedure taken from Refs. 17-19. Basically, a mixture of CdO, Oleic Acid, and Octadecene is heated up to 300°C to allow decomposition of CdO and formation of Cadmium oleate until a clear solution is obtained. A second mixture of Se, trioctylphosphine and Octadecene is heated up to 150°C and kept at constant temperature until a clear yellow solution is observed, indicating the formation of a TOP-Se complex. The selenium solution is then cooled down to room temperature and rapidly injected into the hot cadmium solution. The temperature of the final mixture is set at 280°C to allow crystal growth. The solution undergoes a slow change in color from pale yellow to dark wine red, directly indicating CdSe particle formation and growth. The reaction is stopped when the desired nanocrystal size is reached. All the synthesis is carried out under argon atmosphere. Figure 2 shows the linear spectra for two different samples, CdSe-590 (concentration = 5.80 g/L, R = 2.4 ± 0.5nm) and CdSe-555 (concentration = 4.7 g/L, R = 2.1 ± 0.3nm). While CdSe-590 is dispersed in Octadecene, CdSe-555 is dispersed in Methanol.

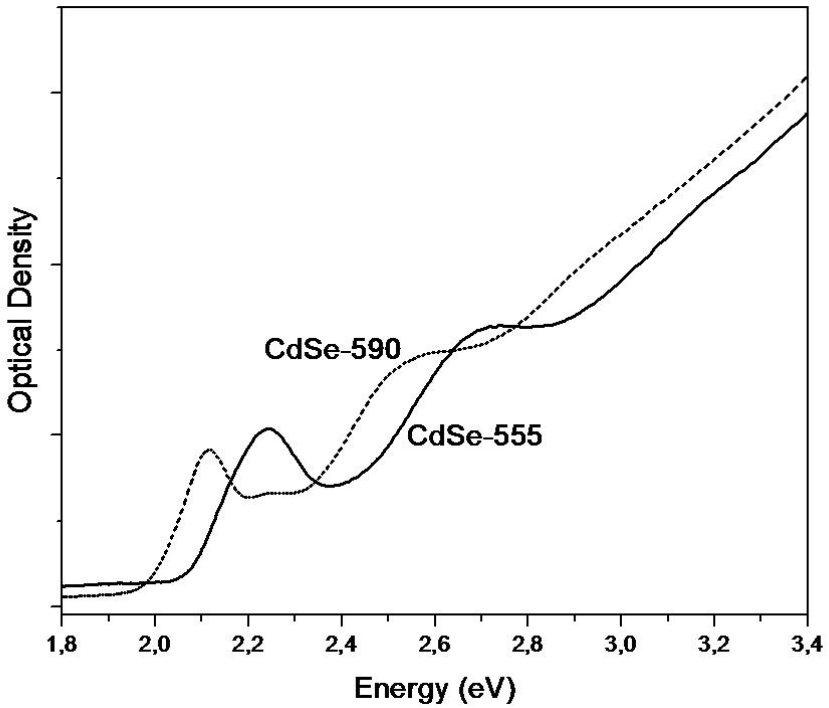

Fig. 2 Linear absorption spectra for the CdSe QDs.

2.2 Experimental Setups

The degenerate 2PA is measured by open aperture Z-scans[13] for the CdTe samples, and by 2PF[15] for the CdSe samples. We chose two different experiments because for Z-scan it is necessary to use high concentration solutions, and the CdSe sample concentration is about 10^{-3}, one order of magnitude lower than the CdTe samples. Also, for 2PF it is necessary to have a high quantum yield that is high enough only for the CdSe samples. To determine the spectrum, we run the Z-scan and the 2PF experiments at different wavelengths using an optical parametric generator/amplifier (OPA) tunable from 500 nm up to 2.2 μm, which generates femtosecond pulses with ~140fs FWHM. The OPA is pumped by a 1mJ, 1kHz Ti:sapphire regenerative amplifier laser system at 775nm.

The nondegenerate 2PA spectra were measured by a white light continuum (WLC) pump-probe technique[14] for all four samples. In this experiment the pump beam is generated by an OPA identical to that used for the Z-scan and 2PF measurements, and the probe beam is a WLC generated in a CaF_2 crystal pumped by another OPA at 1300 nm. Spectral bandpass filters, with ~10 nm spectral band and central wavelength at ω_1, are used for selecting the probe wavelength so that we are able to study the absorption of the probe photon, with energy $\hbar\omega_1$, due to the presence of the pump photon, with energy $\hbar\omega_2$. Using bandpass filters with different ω_1 we can cover a broad spectrum for the nondegenerate 2PA for a

given pump photon energy. The pump photon energy is chosen to be lower than ½ E_g, (E_g is the bandgap energy) and the probe beam is made weak enough so that the influence of any degenerate 2PA is negligible.

3. EXPERIMENTAL RESULTS

3.1 Degenerate two-photon absorption

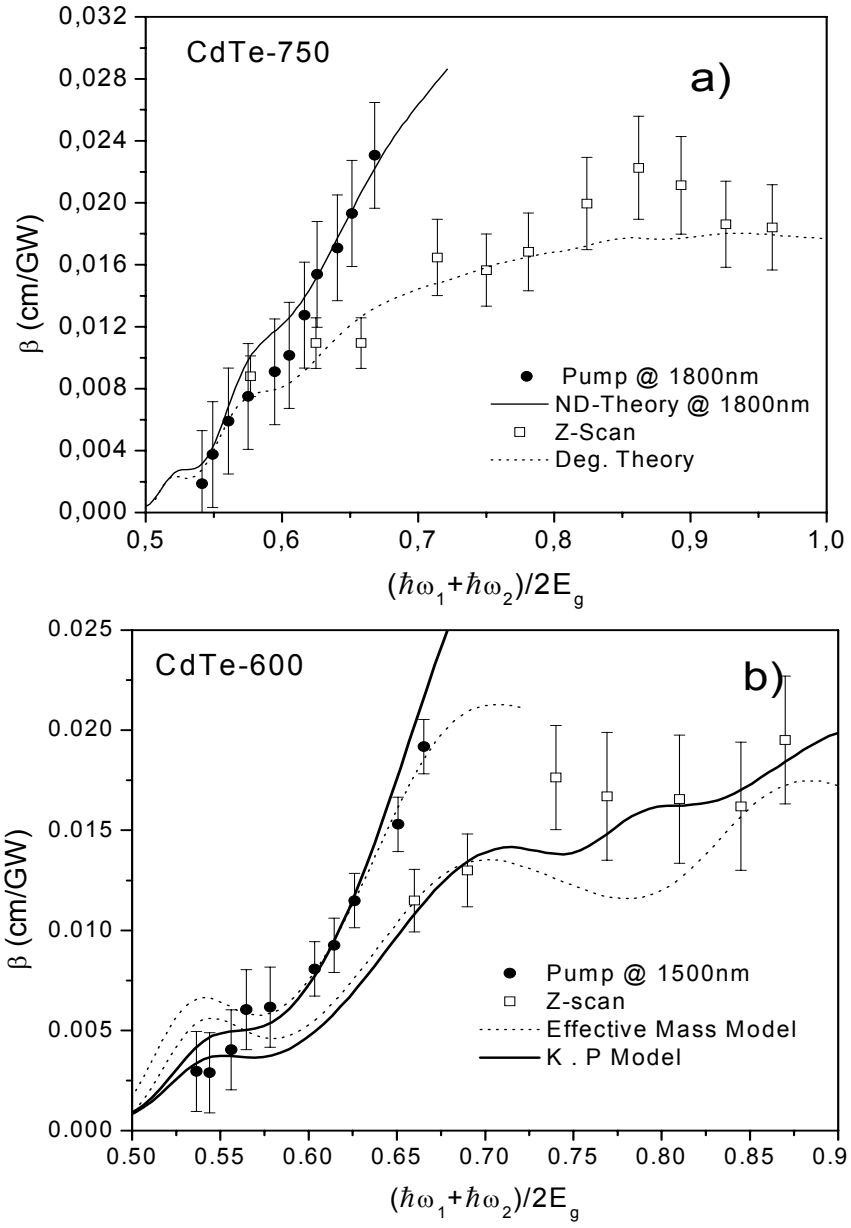

Fig. 3 Degenerate and nondegenerate 2PA for CdTe QDs samples

Figure 3 shows the experimental degenerate and nondegenerate 2PA spectra for the two CdTe QDs samples, CdTe-600 and CdTe-750. For the sample CdTe-750 the nondegenerate measurements were taken with the pump fixed at 1800 nm, and for CdTe-600 at 1500nm. This figure shows the difference in the 2PA spectra for different QD sizes. This difference can also be seen in the CdSe samples. Figure 4 compares the degenerate and nondegenerate 2PA spectra for two different CdSe QD sizes. For both CdSe QD samples the nondegenerate measurements were taken with the pump fixed at 1400 nm.

The theoretical fitting shown in Figure 3 are performed by using an effective mass approximation theory previously proposed[10] and for the sample CdTe-600 a model considering the $\vec{k} \cdot \vec{p}$ Hamiltonian[6,20] is also used. The effective mass theory considers four parabolic and independent bands for the semiconductors and the two-photon transition consisting

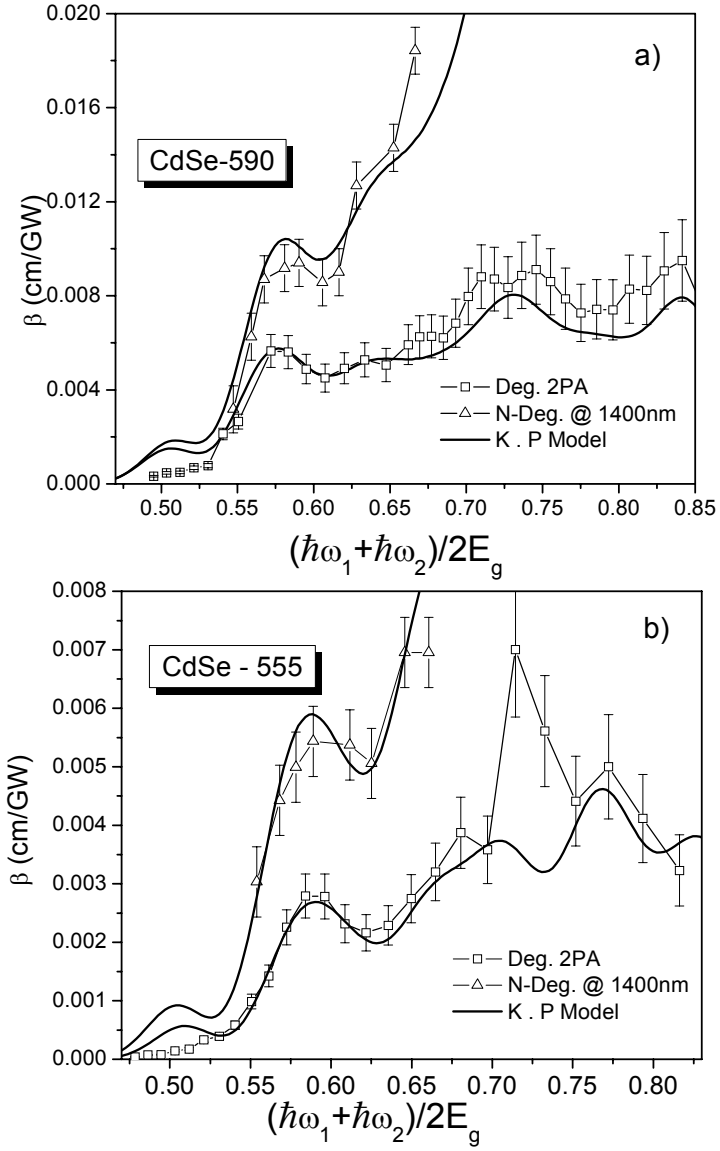

Fig. 4 Degenerate and nondegenerate 2PA for CdSe QD samples

of one intraband and one interband transition. Good agreement is seen the for the largest QDs (CdTe-750) except at the lowest photon energies, however, the theory fails for fitting the spectra for the smaller QDs, especially in the higher energy region.

Sercel and Vahala[6] showed the importance of considering the light and heavy-hole band mixing for the description of the electronic structures in semiconductor QDs. That mixing is obtained by considering the Kane $\vec{k} \cdot \vec{p}$ Hamiltonian[21] and solving the problem to first order in $\vec{k} \to 0$. This breaks the symmetry of the wave functions and allows some transitions that are forbidden in the effective mass model. Because of this, the oscillator strength of the two-photon transition changes. Also, considering the band mixing, the band structure changes and the position of the transition peaks are not the same as those predicted by the effective mass approximation.

For the $\vec{k} \cdot \vec{p}$ model, we consider the mixing between the light and heavy-hole bands, and we neglect any mixing of those bands with the split-off band and with the electronic conduction band. This approximation is valid as long as the difference in energies of the states in the same band is smaller than the split-off energy, Δ, and the bandgap energy, E_g. With these considerations, in this model, the states are written as linear combinations of different spherical Bessel functions, and the energies are no longer defined by zeros of single spherical Bessel functions [6,22]. Therefore additional transitions are allowed, other than those predicted by the effective mass model,[10] e.g. intraband transitions. The good quantum numbers are $\vec{F}$ and F_z, the total angular momentum and its projection in the z direction.

Different from the effective mass approximation[10], the model considering the $\vec{k} \cdot \vec{p}$ approximation does not have an analytical expression for the 2PA transitions in QDs, and each transition has to be calculated separately. However, for fitting the experimental data it is necessary to multiply the result by an overall scaling parameter, *K*, in the same way as was done for the effective mass approximation[10,11]:

$$\beta(x_1, x_2) = \frac{N}{x_1 x_2^2} K^2 \left\langle F^{(2)}(x_1, x_2) \right\rangle \tag{1}$$

where *N* is the QD concentration in the sample, $F^{(2)}(x_1, x_2)$ is the two-photon transition rate, and $x_j = \frac{\hbar \omega_j}{E_g}$. For the degenerate case, one sets $\omega_1 = \omega_2 = \omega$. The parameter *K* has to be the same for different sizes of QDs and for different processes, degenerate or nondegenerate.

In Figure 4 all the fittings are done by the $\vec{k} \cdot \vec{p}$ approximation showing good agreement, the best for sample CdS-590. For the smaller sized QDs of sample CdSe-555 this model does not fit as well for the higher photon energy range suggesting that the mixing of the split-off band has to be considered.

Also, for fitting both CdSe-590 and CdSe-555 the *K* values, Eq. (1), used are *K*=0.42 for CdSe-590 and *K*=0.36 for CdSe-555. The discrepancy of the *K* values indicates that the reduction of the 2PA absorption for smaller QDs experimentally observed is more pronounced than that predicted by the theoretical model.

Figure 5 shows the degenerate 2PA normalized by concentration for the CdTe and CdSe QD samples. We can see that the maximum value for the 2PA coefficient for the CdTe-600 is smaller than the value measured for CdTe-750 and the same trend is verified for the CdSe samples.

The theory predicts that the oscillator strength for each allowed 2-photon transition increases as the QD size decreases. However, the decreasing in the overall values for smaller nanocrystals is due to a reduction of the number of possible transitions, mainly for the high energy range, and to the blue shift in the bandgap introduced by the quantum confinement.

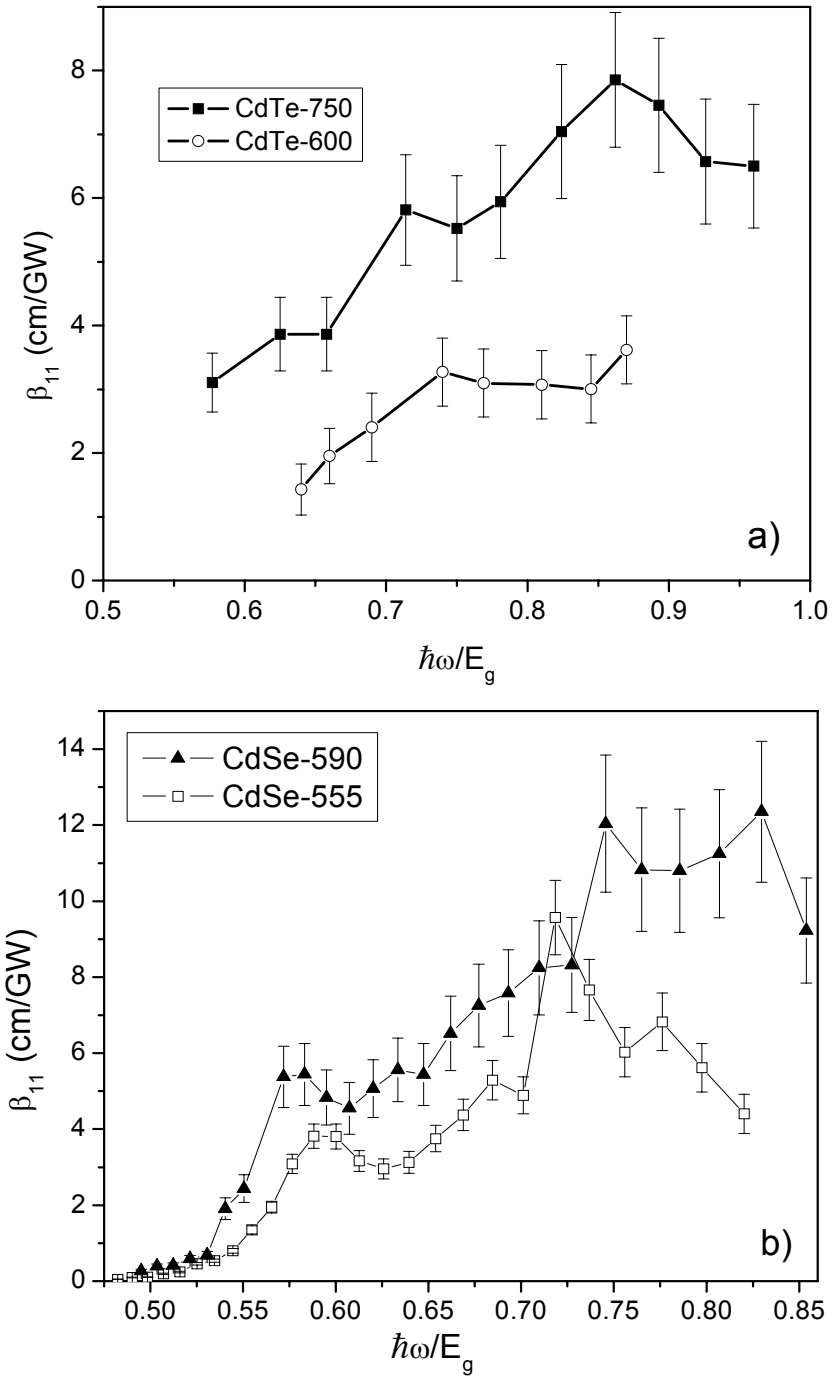

Fig. 5 Comparing the 2PA spectra for different sizes of a) CdTe, and b) CdSe QDs.

4. CONCLUSIONS

The degenerate and nondegenerate two-photon absorption spectra were studied in two different sizes of CdTe and CdSe QDs. The measurements confirm previous results that the spectra depend on the QD size and that smaller QDs present lower two-photon absorption coefficients, β. Including the light and heavy-hole band mixing, we show some

improvement in the theoretical fitting. However, one can see that even the more complete model fails for the smallest QDs. For a given two-photon transition, the oscillator strength is inversely proportional to the QD radius, which suggests stronger 2PA processes for smaller QDs. However, a reduction is observed in the 2PA coefficient for smaller QDs, and this can be explained in part by the blue shift in the band gap introduced by the confinement and by the reduction in the density of possible transitions.

ACKNOWLEDGEMENTS

L. A. Padilha thanks CAPES and FAPESP (Brazilian agencies for funding science) for financial support. We also gratefully acknowledge the support of the National Science Foundation ECS 0217932, the US Army Research Laboratory, and the Army Research Laboratories,

REFERENCES

1. D.R. Larson, W.R. Zipfel, R.M. Willians, S.W. Clark, M.P. Bruchez, F.W. Wise, W.W. Webb, *Science* 300, pp 1434-1436 (2003)
2. E.H. Sargent, *Adv. Matt.* **17**, pp. 515-522 (2005).
3. L.A. Padilha, A.A.R. Neves, E. Rodriguez, C.L. Cesar, L.C. Barobosa, C.H.B. Cruz, *Appl. Phys. Lett.* **86**, pp. 161111-1 – 161111-3 (2005).
4. A. V. Uskov, E. P. O'Reilly, R. J. Manning, R. P. Webb, D. Cotter, M. Laemmlin, N. N. Ledentsov, and D. Bimberg, *IEEE Phot. Tech.. Lett* **16**, pp. 1265-1267 (2004).
5. V. Cerletti, W.A. Coish, O Gywat, and D. Loss, *Nanotech.* **16**, pp. R27-R49 (2005).
6. P. C. Sercel and K. J. Vahala, *Phys. Rev. B* **42**, pp. 3690-3710 (1990).
7. D. Cotter, M.G. Burt, and R.J. Manning, *Phys. Rev. Lett.* **68**, pp. 1200-1203 (1992).
8. J. T. Seo, Q. Yang, S. Creekmore, D. Temple, L. Qu, W. Yu, A. Wang, X. Peng, A. Mott, M. Namkung, S. S. Jung, J. H. Kim, *Phys. E* **17**, pp. 101-103 (2003).
9. G. P. Banfi, V. Degiorgio, and D. Ricard, *Adv. Phys.* **47**, pp. 447-510 (1998).
10. L.A. Padilha, J. Fu, D.J. Hagan, E.W. Van Stryland, C.L. Cesar, L.C. Barbosa, and C.H. Brito Cruz, *Opt. Exp.* **13**, pp. 6460-6467 (2005).
11. L.A. Padilha, J. Fu, D.J. Hagan, E.W. Van Stryland, C.L. Cesar, L.C. Barbosa, and C.H. Brito Cruz, *Proc. SPIE* **5931**, pp. 226-235 (2005).
12. A.V. Fedorov, A.V. Baranv, and K. Inoue, *Phys. Rev. B* **54**, pp. 8627-8632 (1996).
13. M. Sheik-Bahae, A. A. Said, T. H. Wei, D. J. Hagan, and E. W. Van Stryland, *IEEE J. of Quantum Electron.* **26**, pp. 760-769 (1990).
14. R. A. Negres, J. M. Hales, A. Kobyakov, D. J. Hagan, and E. W. Van Stryland, *IEEE J. Quantum Electron.* **38**, pp. 1205-1216 (2002).
15. J.M. Hales, D.J. Hagan., E.W. Van Stryland, K.J. Schafer, A.R. Morales, K.D. Belfield, P. Pacher, O. Kwon, E. Zojer, and J.L. Bredas, *J. Chem. Phys.* **121**, pp. 3152-3160 (2004).
16. L.C. Barbosa, V.C.S. Reynoso, A.M. de Paula, C.R.M. de Oliveira, O.L. Alves, A.F. Craievich, R.E. Marotti, C.H.B. Cruz, and C.L. Cesar, *J. Non-Cryst. Solids* **219**, pp. 205-211 (1997).
17. W.W. Yu, L.H. Qu, W.Z. Guo, and X.G. Peng, *Chem. Mater.* **15**, 2854 (2003).

18. S.D. Bunge, K.M. Krueger, T.J. Boyle, M.A. Rodriguez, T.J. Headley, and V.L. Colvin, *J. Mater. Chem.* **13**, 1705 (2003).

19. L.H Qu and X.G. Peng, *J. Am. Chem. Soc.* **124**, 2049 (2002).

20. L.A. Padilha, J. Fu, D.J. Hagan, E.W. Van Stryland, C.L. Cesar, L.C. Barbosa, C.H.B. Cruz, D. Buso, and A. Martucci, to be published (2006).

21. E.O. Kane, *Semiconductors & Semimetals*, v.1, Cap. 3.

22. A.I. Ekimov, F. Hache, M.C. Schanne-Klein, D. Richard, C. Flytzanis, I.A. Kudryavtsev, T.V. Yazeva, A.V. Rodina, and Al.L. Efros, *J. Opt. Soc. Am. B* **10**, pp. 100-107 (1993).